Geochemistry Geophysics Geosystems G3
AN ELECTRONIC JOURNAL OF THE EARTH SCIENCES
Published by AGU and the Geochemical Society

Technical Brief
Volume 8, Number 5
26 May 2007
Q05013, doi:10.1029/2006GC001521
ISSN: 1525-2027

Fifth-generation lithospheric magnetic field model from CHAMP satellite measurements

Stefan Maus
CIRES, University of Colorado, and NOAA's National Geophysical Data Center, 325 Broadway, Boulder, Colorado 80305, USA (stefan.maus@noaa.gov)

Hermann Lühr and Martin Rother
GFZ Potsdam, Telegrafenberg, D-14473 Potsdam, Germany

Kumar Hemant
School of Earth and Environment, University of Leeds, Leeds LS2 9JT, UK

George Balasis
National Observatory of Athens, Metaxa Str., Penteli, GR-15236 Athens, Greece

Patricia Ritter and Claudia Stolle
GFZ Potsdam, Telegrafenberg, D-14473 Potsdam, Germany

[1] Six years of low-orbit CHAMP satellite magnetic measurements have provided an exceptionally high-quality data resource for lithospheric magnetic field modeling and interpretation. Here we describe the fifth-generation satellite-only magnetic field model MF5. The model extends to spherical harmonic degree 100. As a result of careful data selection, extensive corrections, filtering, and line leveling, the model has low noise levels, even if evaluated at the Earth's surface. The model is particularly suited for inferring large-scale structure and composition of the lithosphere. It is also meant to serve as the long-wavelength part of continental- and global-scale marine and aeromagnetic anomaly maps.

Components: 4281 words, 2 figures, 2 tables.

Keywords: geomagnetic field; crustal field; satellite geomagnetism.

Index Terms: 1541 Geomagnetism and Paleomagnetism: Satellite magnetics: main field, crustal field, external field; 1545 Geomagnetism and Paleomagnetism: Spatial variations: all harmonics and anomalies; 1532 Geomagnetism and Paleomagnetism: Reference fields: regional, global.

Received 1 November 2006; **Revised** 19 January 2007; **Accepted** 12 February 2007; **Published** 26 May 2007.

Maus, S., H. Lühr, M. Rother, K. Hemant, G. Balasis, P. Ritter, and C. Stolle (2007), Fifth-generation lithospheric magnetic field model from CHAMP satellite measurements, *Geochem. Geophys. Geosyst.*, *8*, Q05013, doi:10.1029/2006GC001521.

1. Introduction

[2] After a period of 20 years without high-quality, low-orbit satellite magnetic coverage since Magsat (1979–1980), a new generation of satellites is measuring the magnetic field with unprecedented accuracy and resolution. Two satellites were launched into 800 km and 700 km altitude orbits,

namely Ørsted (launched in 1999 and still providing scalar data) and SAC-C (launched in 2001, scalar magnetometer active until 2004), respectively, while the CHAMP satellite was launched in July 2000 into a lower orbit, initially at 450 km altitude. In contrast to earlier satellites, the heavy CHAMP satellite with its small cross-section has the ability to remain at low orbital altitudes for an extended period of time. As of September 2006, CHAMP has descended to about 350 km altitude and the mission is expected to last into 2009. The low altitude of CHAMP at solar-minimum conditions offers extraordinary opportunities for resolving the lithospheric magnetic field. This is further supported by the small polar gap (2.3° radius) and data availability of close to 100%. Finally, CHAMP's dual-head star trackers are the key to providing the cleanest magnetic vector data ever collected in low-Earth orbit.

[3] Presently, several different kinds of geomagnetic field models are produced by different groups. The most general type is the Comprehensive Model [*Sabaka et al.*, 2004]. It parameterizes the major sources of the field, including the core, crust, ionosphere and magnetosphere. The model parameters were estimated in a single grand inversion of all available satellite and magnetic observatory data. However, this model has not been updated since 2002 and does not include CHAMP vector data.

[4] The grand inversion approach has the disadvantage that noisy dayside data have to be included, with the consequence that weaker sources, like the small-scale lithospheric field or the high-degree secular variation, are not well resolved. For our latest lithospheric field model MF5 we therefore take a different approach and select the most quiet nighttime data, after applying suitable corrections for unmodeled field contributions.

[5] We would like to point out the particular relevance of MF5 in combining satellite with marine and aeromagnetic anomaly maps. Such near-surface anomaly maps display the residual of the magnetic field strength after subtracting a main field model. They have played a large role in developing the theory of plate tectonics and understanding lithospheric structure and composition. When merging individual aeromagnetic and marine surveys, typically extending over a couple of hundred kilometers, one faces the difficulty that the long wavelengths of the resulting compilations are not well constrained. Satellites are well suited to supply the missing large-scale picture, for instance, by filtering magnetic compilations with a 400 km cut-off wavelength and substituting the long wavelengths from a satellite-based model. There are now efforts underway to produce a global magnetic anomaly map [*Maus et al.*, 2007]. The project is coordinated by the task force for the World Digital Magnetic Anomaly Map (WDMAM) of the International Association for Geomagnetism and Aeronomy (IAGA). One of the main aims in producing the model MF5 was to provide the long wavelength magnetic field for this project.

2. Data Processing and Model Estimation

[6] The MF series of magnetic field models is strictly focused on the lithospheric field. Our initial model MF1 [*Maus et al.*, 2002] was only determined from scalar (total intensity) data, acquired during the first year of the CHAMP mission. This model, and its revisions MF2 and MF3 which made use of CHAMP vector data, are available at http://www.gfz-potsdam.de/pb2/pb23/SatMag/model.html. Our fourth-generation lithospheric field model MF4 [*Maus et al.*, 2006b] was based on further improvements in the processing methodology. For the first time, a line-leveling technique was used in order to reduce across-track noise. Nevertheless, MF4 still contains small-scale noise at high latitudes which becomes visible when the model is downward continued all the way to the Earth's surface. This problem was overcome in model MF4x [*Lesur and Maus*, 2006], which used the same (cleaned and line-leveled) input data as MF4, but with a different coefficient estimation scheme. By using combinations of spherical harmonics, *Lesur* [2006] defined basis functions with local support which were used to produce a model with degree-90 resolution at lower latitudes and degree-60 resolution in the Polar Regions. The only disadvantage of this approach is that the model no longer has a well-defined cut-off wavelength. This becomes a problem when merging satellite and near-surface data. If one were to substitute degrees 1–90 of a global near-surface magnetic compilation with MF4x, the result would have deficient power in the wave band of degrees 60–90. For MF5, we therefore aimed at producing a model which was as noise-free as possible up to degree 100, corresponding to 400 km wavelength at the Earth's surface.

[7] The new MF5 model was produced in a very similar way to the MF4 model. To keep the model

Table 1. Number of Vector and Scalar CHAMP Measurements Used in This Study[a]

	South Polar	Middle Latitude	North Polar
Vector		2,747,000	
Scalar	464,000	3,780,000	427,000

[a] South polar tracks are below −55°, north polar are above 55°, middle latitude scalar tracks cover the overlapping range of −65° to 65°, and middle latitude vector tracks range from −55° to 55° magnetic latitude.

as noise-free as possible, even at high latitudes, we implemented two improvements: The first was to use only the latest three years of CHAMP scalar and vector measurements. This has the advantage of a lower flight altitude. But it also makes the altitude distribution more homogeneous. CHAMP was lifted several times in the past years, and its orbit has become even less eccentric. This homogeneous altitude distribution helps in the second improvement, better line leveling. In the following, we give a step-by-step description of the processing scheme.

2.1. Data Selection

[8] At satellite altitude the amplitude of the lithospheric field is very small, in particular that of the small-scale features. To isolate this signature, the first step is therefore to select the least-disturbed data. Since the properties of low- and high-latitude data are quite different, we selected and processed these data separately. In the following, we define the middle-latitude vector data as ranging from −55° to 55° magnetic latitude, the middle-latitude scalar data from −65° to 65°, and the overlapping high-latitude scalar data as <−55° and >55° magnetic latitude. No vector data were used at high latitudes. The final data numbers are given in Table 1.

[9] At middle latitudes we selected data from the 20:00 to 05:00 local time interval with Kp $\leq$ 2. The post-sunset equatorial ionosphere is susceptible to local plasma irregularities forming so-called plasma bubbles, which cause systematically positive magnetic deflections of up to 5 nT in field strength [*Balasis et al.*, 2005]. Contaminated tracks were identified here by an automatic detection process and have been discarded. Herein, the field magnitude of the single tracks was high-pass filtered with a cut-off period of 30 s (230 km). The filtered tracks were checked for peaks higher than ±0.25 nT. Plasma instabilities were identified if neighboring peaks within a 6° latitudinal window were also found. The occurrence rate of contaminated tracks was found to vary from 0% – 80% depending on longitude, season and local time. A more detailed description of the detection process and the climatology of magnetic signatures due to plasma bubble activity was given by *Stolle et al.* [2006].

[10] At high latitudes neither local time nor Kp are suitable selection criteria. We have partly relied on a set of tracks identified as undisturbed in an analysis by *Ritter and Lühr* [2006]. Additional tracks were included which satisfy similar criteria, namely a merging electric field at the magnetopause of E_m < 0.8 mV/m and Interplanetary Magnetic Field (IMF) conditions with |IMF B_y| < 8 nT and −2 nT < IMF B_z < 6 nT. Disturbances by field-aligned currents were avoided by using only scalar data at high latitudes.

2.2. Main and Magnetospheric Field Subtraction

[11] To remove contributions to the magnetic field from the Earth's core and magnetosphere, we subtracted the field model POMME-3.0 [*Maus et al.*, 2006c], with the static part of the internal field limited to SH degree 15. This correction also includes terms accounting for fields due to currents induced in the Earth by time-varying magnetospheric fields [*Maus and Lühr*, 2005].

2.3. Ocean Tidal Flow

[12] Flow of conducting seawater through the Earth's magnetic field induces currents which in turn give rise to secondary magnetic fields. For tidal flow, these signals reach amplitudes of 3 nT at 400 km altitude and are clearly identified in magnetic satellite data [*Tyler et al.*, 2003]. Since tidal ocean flow is well determined from satellite altimetry, a rather accurate prediction of its magnetic signal can be made [*Kuvshinov and Olsen*, 2005]. Subtracting the predicted magnetic fields for the eight major tidal constituents almost completely removes the tidal signal from the magnetic residuals, as can be seen in the temporal power spectrum [*Maus et al.*, 2006b, Figure 2].

2.4. *F* Region Currents at Low Latitudes

[13] While the ionospheric *E* region (90–130 km altitude) becomes non-conducting during dark hours, the ionospheric *F* region (above 130 km)

retains considerable plasma density during the night. Two types of currents in the *F* region have been corrected for here:

[14] Plasma pressure-driven electric currents reduce the magnetic field in the equatorial ionospheric anomaly on both sides of the magnetic equator by a few nT. This effect is particularly important for CHAMP, with its orbital altitude close to the peak ionospheric plasma density. Using the electron density and temperature measurements from the Langmuir Probe, the magnetic field readings of CHAMP were corrected using the approximate formula for the diamagnetic effect given by *Lühr et al.* [2003].

[15] The gravity-driven current system in the ionospheric *F* region generates a significant magnetic signal of the order of 5 nT. For its correction we used the ion densities from the International Reference Ionosphere, IRI-2000 [*Bilitza*, 2001], and determined the primary gravity-driven current on 46 horizontal shells with a vertical spacing of 20 km. For each shell, we then found the nondivergent, freely flowing part of the current. Integrating over the magnetic effects of the currents in all shells, we obtained the magnetic signal at the measurement locations along the satellite orbit. Further details of the correction are given by *Maus and Lühr* [2006].

2.5. Polar Electrojets

[16] Even during magnetically quiet periods Polar electrojets (PEJs) have signal strengths of the order of 50 nT at 400 km altitude. Nevertheless, there are occasional tracks in which the PEJ are negligible. Due to the dense coverage over the Polar Regions, enough of such quiet tracks can be found at high latitudes so that a correction for PEJ fields is not necessary. The situation is different for middle latitudes, where one cannot afford to discard 98% of the tracks.

[17] The main PEJ current axis is located on average at about ±70° magnetic latitude. An appreciable part of the related magnetic fields can be sensed quite far down to low latitudes. This far field effect cannot be considered as random noise because the PEJs are preferably directed from the day to the night side. Hence, during the local time interval of 20:00 to 05:00 used here, they flow primarily westward and generate a reduction in the ambient field magnitude at middle latitudes, in the northern as well as the southern hemisphere. In order to avoid spurious negative anomalies at about 50° to 65° north and south magnetic latitude, we corrected for the signal of the PEJs. This was done by introducing one parameter each for the northern and southern PEJ intensity and co-estimating these two parameters in the along-track filtering described below. Further details of the PEJ correction are given by *Maus et al.* [2006b].

2.6. Along-Track Filtering

[18] Even after careful data selection and applying various corrections, one still faces systematic offsets between neighboring tracks. Most of this noise is due to unmodeled contributions from magnetospheric currents, in particular the ring current, and their induction [*Maus et al.*, 2002, Figure 2]. The noise is predominantly of long wavelength and can therefore be removed to a large extent by fitting and subtracting a degree-1 model on a track-by-track basis. One would obtain even cleaner data by also including higher degree internal and external field terms in the track-by-track filtering. However, this would lead to the removal of genuine lithospheric signal, which is of course to be avoided.

[19] For vector data, general degree-1 fields are characterized by 3 external and 3 internal field parameters. In addition, we solve for a set of angles accounting for a remaining uncertainty in the satellite attitude. Since the vector data only extend to ±55° latitude, a PEJ correction was not included. All in all, this gives 9 parameters estimated for each track in the filtering of the vector data.

[20] Scalar data are not sensitive to the components of the magnetic field which are perpendicular to the main field. The main field resembles approximately that of an axial dipole and the CHAMP orbital plane is closely aligned with the magnetic meridian. Therefore only 2 of the 3 components of an external dipole can be resolved by scalar data: one parallel to the main field dipole and one perpendicular, lying within the orbital plane. Two corresponding induced internal dipole coefficients can be defined. However, since the external perpendicular dipole component turns out to be rather small, its induced counterpart should be even smaller. We have therefore omitted it in the cleaning procedure. For high-latitude scalar data, we only fitted these 3 parameters (2 external and one internal). At middle latitudes we further included the intensities of the PEJs, resulting in five parameters estimated for each midlatitude scalar track.

2.7. Line Leveling

[21] Despite the various measures to isolate the lithospheric signal by data selection, subtraction of models for the various contributions, and filtering, significant non-lithospheric contributions remain in the data. In particular, this noise leads to arbitrary offsets between adjacent tracks. These offsets can be reduced by minimizing the difference between neighboring tracks and at cross-over points between ascending and descending tracks.

[22] Our line-leveling algorithm minimizes the distance-weighted misfit of the residuals against MF4x [*Lesur and Maus*, 2006], between all nearest pairs of measurements for all pairs of tracks. To account for stronger variation in the vertical direction, vertical distances are up-weighted. The exact weight function is given by *Maus et al.* [2006b].

[23] As for MF4, the scalar data sets from the three latitude ranges (North Pole, South Pole and middle latitudes) were first leveled against each other. Then the vector data were leveled onto the scalar data. In contrast to along-track filtering, where higher degree filters lead to a loss of genuine signal, minimizing offsets between tracks does not appear to remove a significant amount of lithospheric signal. For MF4, we took a conservative view of this issue and used only corrections up to SH degree 3. For MF5 we used corrections up to degree 20 for high-latitude scalar data, degree 12 for middle-latitude scalar data, and degree 6 for middle-latitude vector data. There is a danger of suppressing genuine lithospheric signal when applying adjustments that are of wavelengths overlapping with the crustal field. This is in particular the case for the degree 20 correction which we used at high latitudes. However, if several tracks consistently exhibit the same features, the line leveling does not suppress them. This is in contrast to the above-described along-track filters, which completely remove the signal in the effective wave band. The line leveling resulted in a very clean input data set for the following high-degree model coefficient estimation.

2.8. Least Squares Estimation of Gauss Coefficients

[24] The data were weighted in such a way as to give equal cumulative weight to every unit area on the sphere, by counting data numbers in equal-area bins and down-weighting them by the number density. Then, the spherical harmonic coefficients of the scalar potential representing the lithospheric magnetic field were estimated to degree and order 100 using the standard least squares approach described by *Maus et al.* [2006b].

2.9. Regularization

[25] In the least squares model estimation, some higher degree coefficients are affected by noise, or are less well constrained by the data and tend to "blow up." While this problem started at degree 60 for the MF4 model, the coefficients up to degree 80 appear to be well determined in MF5. Above degree 80 there are groups of coefficients which are contaminated by noise, resulting in systematically increased power. Such clusters of coefficients with increased power were damped by a procedure which is described in detail by *Maus et al.* [2006b].

3. Result

[26] The final MF5 model is shown in Figure 1, where it is compared at ground level with earlier models of the MF series. At first sight, it is difficult to distinguish genuine from spurious anomalies. However, there are often strong anomalies at the ocean/continent boundaries. If one focuses on these, the difference between true anomalies and noise becomes evident.

[27] Extending up to SH degree 100, the MF5 model shows a higher level of detail than MF4 and MF4x. This is apparent even at middle latitudes. Particularly interesting is the comparison in the Antarctic region. The MF4 model has high noise levels over the oceanic crust between Antarctica and Australia (90° to 180° longitude). This is a region which is right under the polar electrojets and therefore particularly difficult to map. The noise in MF4 was avoided in MF4x by extending the local basis functions only up to degree 60 in the high-latitude regions. However, that resulted in a significant loss of detail. By using lower-altitude CHAMP observations and more effective data cleaning, it was possible to produce the MF5 model with the full degree-100 resolution without introducing significant noise in that region.

[28] The residuals of the input data against the model are summarized in Table 2. However, these residuals are not statistically independent, but spatially correlated. Figure 2 therefore shows maps of the fit of the model to the input data. The residuals of the vector components are much stronger than the residuals of the scalar data. The high vector

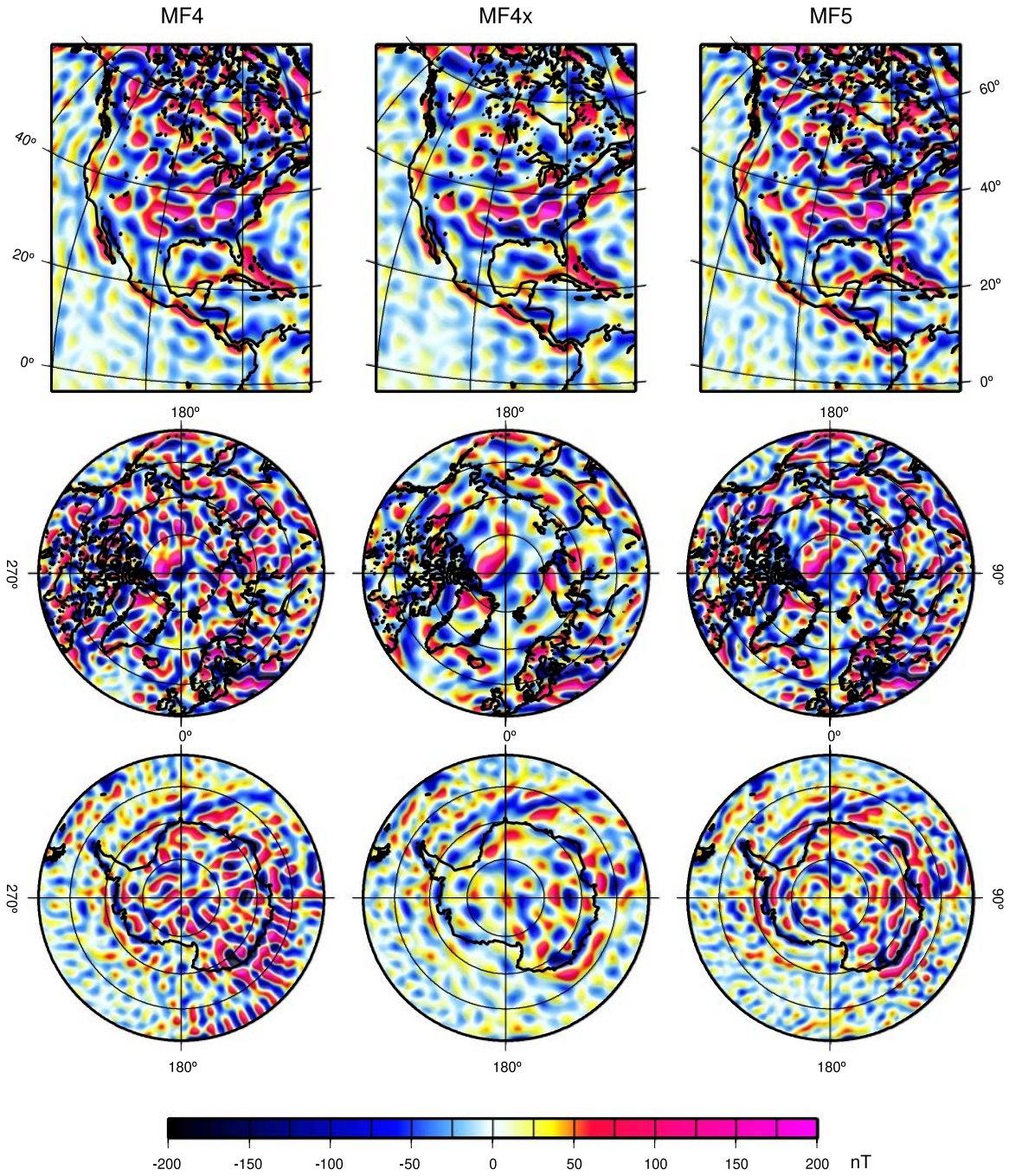

Figure 1. A comparison of the new MF5 model (right side) with MF4 (left) and MF4x (middle) at low and high latitudes.

residuals are partly due to uncertainties in the satellite attitude, and partly a consequence of unmodeled external fields. The large-scale pattern following the magnetic equator indicates that our correction for gravity-driven ionospheric currents requires further improvement. However, these large-scale biases are not likely to significantly affect the model, which only has SH coefficients of degree 16 and higher. In the scalar residuals the large-scale, equator-parallel pattern is much weaker. Instead, there are small-scale patterns which are most prominent over the continents,

Table 2. Summary of Root Mean Square Data Residuals Against the Final Model[a]

	South Polar	Middle Latitude	North Polar
X		0.95	
Y		0.88	
Z		1.1	
F	0.25	0.28	0.44

[a] Data residuals are in nT. X refers to the northward component, Y refers to the eastward component, Z refers to the downward component, and F refers to the total intensity of the field.

particularly over areas of strong lithospheric magnetization. These "ringing" patterns are most likely caused by the abrupt truncation of the model at SH degree 100. Since this residual small-scale signal is encouragingly clear, it may be possible to extend the next generation of the MF model series to a significantly higher degree.

[29] The model coefficients are archived at http://earthref.org/cgi-bin/erda.cgi?n=720. Further material, including grids, images and animations are available at our Web sites http://models.geomag.us/MF5.html and http://www.gfz-potsdam.de/pb2/pb23/SatMag/litmod5.html.

4. Outlook

[30] Lithospheric magnetic field models will experience significant gains in resolution and accuracy over the coming years. The CHAMP mission is expected to continue providing excellent quality data at solar minimum conditions and at steadily decreasing altitudes up to the year 2009. Following in 2010 is the European Space Agency's *Swarm* mission, a constellation comprising 3 satellites (http://www.esa.int/esaLP/LPswarm.html). This will further improve the data basis for mapping lithospheric magnetic anomalies by providing direct measurements of the magnetic field gradient for the analysis [*Maus et al.*, 2006a]. Simultaneously, the WDMAM task force (http://www.ngdc.noaa.gov/IAGA/vmod/) is successfully unearthing previously unavailable near-surface magnetic data sets. Merging these with the large-scale field provided by satellite data will eventually provide a new generation of high-resolution global lithospheric field models.

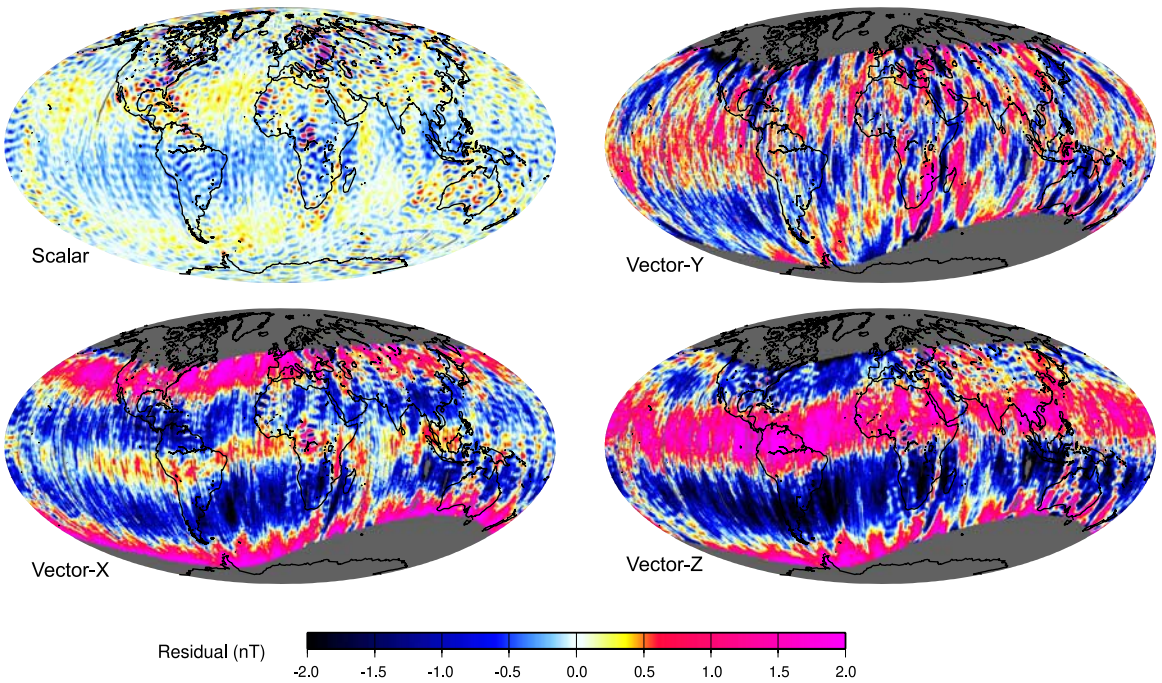

Figure 2. Residuals of the cleaned, filtered, and line-leveled data against the final model (measurement minus model). The scalar residuals appear to be dominated by the model truncation at SH degree 100. In contrast, the vector component residuals (X, northward; Y, eastward; Z, downward) show large-scale systematic patterns which we attribute to inaccurately modeled ionospheric currents.

Acknowledgments

[31] We thank two anonymous reviewers for their valuable comments and suggestions. This work was supported by the Deutsche Forschungsgemeinschaft (DFG) as part of the Special Program "Geomagnetic Field Variations" (SPP 1097). The operational support of the CHAMP mission by the German Aerospace Center (DLR) and the financial support for the data processing by Federal Ministry of Education and Research (BMBF) are gratefully acknowledged.

References

Balasis, G., S. Maus, H. Lühr, and M. Rother (2005), Wavelet analysis of CHAMP flux gate magnetometer data, in *Earth Observation With CHAMP: Results From Three Years in Orbit*, edited by C. Reigber et al., pp. 347–352, Springer, New York.

Bilitza, D. (2001), International Reference Ionosphere 2000, *Radio Sci.*, *36*, 261–275.

Kuvshinov, A., and N. Olsen (2005), 3-D modelling of the magnetic field due to ocean tidal flow, in *Earth Observation With CHAMP: Results From Three Years in Orbit*, edited by C. Reigber et al., pp. 359–365, Springer, New York.

Lesur, V. (2006), Introducing localized constraint in global geomagnetic field modelling, *Earth Planets Space*, *58*, 477–483.

Lesur, V., and S. Maus (2006), A global lithospheric magnetic field model with reduced noise level in the Polar Regions, *Geophys. Res. Lett.*, *33*, L13304, doi:10.1029/2006GL025826.

Lühr, H., M. Rother, S. Maus, W. Mai, and D. Cooke (2003), The diamagnetic effect of the equatorial Appleton anomaly: Its characteristics and impact on geomagnetic field modeling, *Geophys. Res. Lett.*, *30*(17), 1906, doi:10.1029/2003GL017407.

Maus, S., and H. Lühr (2005), Signature of the quiet-time magnetospheric magnetic field and its electromagnetic induction in the rotating Earth, *Geophys. J. Int.*, doi:10.1111/j.1365-246X.2005.02691.x.

Maus, S., and H. Lühr (2006), A gravity-driven electric current in the Earth's ionosphere identified in CHAMP satellite magnetic measurements, *Geophys. Res. Lett.*, *33*, L02812, doi:10.1029/2005GL024436.

Maus, S., M. Rother, R. Holme, H. Lühr, N. Olsen, and V. Haak (2002), First scalar magnetic anomaly map from CHAMP satellite data indicates weak lithospheric field, *Geophys. Res. Lett.*, *29*(14), 1702, doi:10.1029/2001GL013685.

Maus, S., H. Luehr, and M. E. Purucker (2006a), Simulation of the high-degree lithospheric field recovery for the Swarm constellation of satellites, *Earth Planets Space*, *58*(4), 397–407.

Maus, S., M. Rother, K. Hemant, C. Stolle, H. Lühr, A. Kuvshinov, and N. Olsen (2006b), Earth's lithospheric magnetic field determined to spherical harmonic degree 90 from CHAMP satellite measurements, *Geophys. J. Int.*, *164*, 319–330, doi:10.1111/j.1365-246X.2005.02833.x.

Maus, S., M. Rother, C. Stolle, W. Mai, S. Choi, H. Lühr, D. Cooke, and C. Roth (2006c), Third generation of the Potsdam Magnetic Model of the Earth (POMME), *Geochem. Geophys. Geosyst.*, *7*, Q07008, doi:10.1029/2006GC001269.

Maus, S., T. Sazonova, K. Hemant, D. Fairhead, and D. Ravat (2007), National Geophysical Data Center candidate for the World Digital Magnetic Anomaly Map, *Geochem. Geophys. Geosyst.*, doi:10.1029/2007GC001643, in press.

Ritter, P., and H. Lühr (2006), Search for magnetically quiet CHAMP polar passes and the characteristics of ionospheric currents during the dark season, *Ann. Geophys.*, *24*, 2997–3009.

Sabaka, T. J., N. Olsen, and M. E. Purucker (2004), Extending comprehensive models of the Earth's magnetic field with Ørsted and CHAMP data, *Geophys. J. Int.*, *159*, 521–547.

Stolle, C., H. Lühr, M. Rother, and G. Balasis (2006), Magnetic signatures of equatorial spread *F* as observed by the CHAMP satellite, *J. Geophys. Res.*, *111*, A02304, doi:10.1029/2005JA011184.

Tyler, R., S. Maus, and H. Lühr (2003), Satellite observations of magnetic fields due to ocean tidal flow, *Science*, *299*, 239–241.